Journal of Sound and Vibration (1997) **199**(3), 381–400

INSTABILITY ANALYSIS OF UNSYMMETRICAL ROTOR–BEARING SYSTEMS USING THE TRANSFER MATRIX METHOD

Y. KANG, Y.-G. LEE AND S.-C. CHEN

Department of Mechanical Engineering, Chung Yuan Christian University, Chung Li 32023, *Taiwan, Republic of China*

(*Received* 5 *December* 1995, *and in final form* 10 *June* 1996)

In this study, a modified transfer matrix approach, valid for complex rotor–bearing systems, was developed to analyze the instability in unsymmetrical rotor–bearing systems. Specifically, the transfer matrices of non-axisymmetrical shaft segments were derived by using a continuous-system sense to obtain an accurate formulation. The influences of bearing characteristics and shaft asymmetry on the transition curves of T-type and $2T$-type solutions were evaluated by using Bolotin's method.

1. INTRODUCTION

Lateral disturbance in a non-axisymmetrical rotor–bearing system occurs in the resonant modes, even in a perfectly balanced system. A single non-axisymmetrical disk mounted on springs with unequal stiffness along its principal axes was used to study the instability of unsymmetrical rotors in experiments conducted by Crandall and Brosens [1], Yamamoto and Ota [2], Ardayfio and Frohrib [3], and so on. They evaluated the influence of stiffness on instability. The effect of bearing damping was investigated by Rajalingham *et al*. [4] by using a similar model. They demonstrated that the instability can be eliminated by an appropriate choice of bearing parameters and brought a qualitative insight into the relevant phenomena of rotor systems with few degrees of freedom.

Arnold and Haft [5] and Iwatsubo *et al*. [6] analyzed the instability in continuous non-axisymmetrical shafts. Only bending deformation and transverse inertia were considered in their equations, and approximate solutions were obtained in the fixed frame of reference. Lee and Jei [7, 8] presented a modal method for an unsymmetrical rotor–bearing system with general bearing conditions. They performed analyses on continuous equations of shafts in a rotating frame of reference. Genta [9] formulated finite element equations with complex co-ordinates to analyze the behavior of complex unsymmetrical rotors. In particular, unstable regions are obtained from two loci of whirl speeds repelled to each other as the eigenvalue curves of two modes are approaching each other. When the dependence of unstable regions on a system parameter is plotted, a family of eigenvalues must be calculated with various values of this specified parameter.

In addition to the finite element method, the transfer matrix method (TMM) is also an effective implementation for complex rotor–bearing systems. The application of TMM for a stability threshold and damped critical speeds of a flexible rotor was done by Lund [10]. Both the critical speeds and its stability are determined by solving eigenvalues of a damped system. The Newton–Raphson method was used to extract complex eigenvalues. Bansal and Kirk [11] applied the transfer matrix polynomial method to find the instability

0022–460X/97/030381 + 20 $25.00/0/sv960655

threshold and the damped critical speed of a rotor–bearing system. Muller's quadratic interpolation technique was employed to extract the complex roots of the characteristic polynomial equation. Murphy and Vance [12] solved the characteristic polynomial by using Bairstow's method, which can avoid missing some eigenvalues. Kang *et al*. [13] formulated governing equations for a continuous non-axisymmetrical shaft and presented a modified transfer matrix method for the steady state analysis of unsymmetrical rotor–bearing systems.

In this paper a modified transfer matrix method is presented, incorporating Bolotin's method [14], to determine the transition curves of instability in the T- and $2T$-type solutions. The governing equations for non-axisymmetrical Rayleigh shafts, non-axisymmetrical disks and non-axisymmetrical bearings are expressed in a rotating frame of reference. Using modal decoupling, the shaft shape functions of all the resonant modes are derived to formulate the transfer matrix of each shaft. The transition curves of instability are obtained by solving the determinant of the global transfer matrix which satisfies the boundary conditions of both ends of a rotor–bearing system. With one of the system parameters changing and the other parameters remaining constant, the influence of this parameter on instability is calculated in numerical examples. The dependence of bearing characteristics and shaft asymmetry on instability is thus obtained.

2. EQUATIONS OF MOTION

Consider an unsymmetrical rotor–bearing system consisting of flexible non-axisymmetrical Rayleigh shafts, non-axisymmetrical rigid disks and non-axisymmetrical bearings. When the governing equations of the shaft and the disk are expressed in stationary co-ordinates, varying coefficients with double speed frequencies appear in the equations. The problem may be overcome by expressing the governing equations in the rotating co-ordinates instead of the stationary co-ordinates. However, an asymmetry in the boundary condition due to non-axisymmetrical bearings is permitted; i.e., the periodically varying coefficients appear in the governing equations for the bearings expressed in the rotating frame of reference.

2.1. DISK

A non-axisymmetrical and rigid disk, having principal axes μ and v at an angle η apart from the principal axes U and V of the shaft is shown in Figure 1. The equilibrium of moment and shear force of a rigid disk are shown in Figure 2. In the rotating frame of

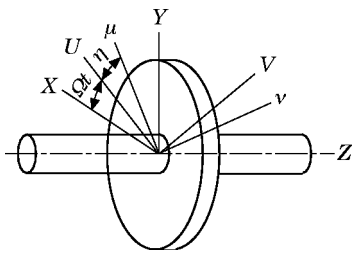

Figure 1. A model of a non-axisymmetrical shaft and disk.

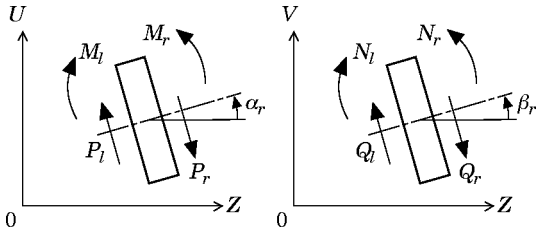

Figure 2. The force and moment equilibrium of a disk.

reference, the equilibrium equations of moments at the disk point can be expressed by (a list of notation is given in Appendix C)

$$\begin{aligned}\mathscr{M}_r &= \mathscr{M}_l + (I^d - \Delta^d \cos 2\eta)\ddot{\alpha} - \Delta^d \ddot{\beta} \sin 2\eta \\ &\quad + \Omega(J^d - 2I^d)\dot{\beta} + \Omega^2(J^d + I^d)\alpha - \Delta^d\Omega^2(\beta \sin 2\eta + \alpha \cos 2\eta), \\ \mathscr{N}_r &= \mathscr{N}_l + (I^d + \Delta^d \cos 2\eta)\ddot{\beta} - \Delta^d \ddot{\alpha} \sin 2\eta \\ &\quad - \Omega(J^d - 2I^d)\dot{\alpha} + \Omega^2(J^d + I^d)\beta - \Delta^d\Omega^2(-\alpha \sin 2\eta + \beta \cos 2\eta),\end{aligned} \tag{1}$$

where $\alpha = \partial U/\partial Z$ and $\beta = \partial V/\partial Z$ are components of the deflected angle about the V- and U-axes, $I^d = (I^d_\mu + I^d_\nu)/2$ and $\Delta^d = (I^d_\mu - I^d_\nu)/2$, and the equilibrium equations of the shear forces can be expressed by

$$\mathscr{P}_r = \mathscr{P}_l - m^d(\ddot{U} - 2\Omega\dot{V} - \Omega^2 U), \qquad \mathscr{Q}_r = \mathscr{Q}_l - m^d(\ddot{V} + 2\Omega\dot{U} - \Omega^2 V), \tag{2}$$

where U and V are components of the lateral displacement along the U- and V-axes. The details of the derivation of equations (1) and (2) are shown in Kang *et al*. [13].

By introducing the non-dimensional quantities, $u = U/L$, $v = V/L$, $z = Z/L$, $\Omega_0 = \pi^2\sqrt{E\Psi/(\rho A)}/L^2$, $M = \mathscr{M}L/E\Psi$, $N = \mathscr{N}L/E\Psi$, $P = \mathscr{P}L^2/E\Psi$, $Q = \mathscr{Q}L^2/E\Psi$, $S_1 = LI^d\Omega_0^2/(E\Psi)$, $S_2 = (\Delta^d/I^d)\cos 2\eta$, $S_3 = (\Delta^d/I^d)\sin 2\eta$, $C_1 = S_1(1 - S_2)$, $C_2 = -S_1S_3$, $C_3 = \gamma^2 S_1(3 - S_2)$, $C_4 = -\gamma^2 S_1 S_3$, $C_5 = S_1(1 + S_2)$, $C_6 = \gamma^2 S_1(3 + S_2)$ and $C_7 = -L^3 m^d \Omega_0^2/(E\Psi)$, equations (1) and (2) become

$$M_r = M_l + C_1\frac{\partial^3 u}{\partial z\,\partial\tau^2} + C_2\frac{\partial^3 v}{\partial z\,\partial\tau^2} + C_3\frac{\partial u}{\partial z} + C_4\frac{\partial v}{\partial z},$$

$$N_r = N_l + C_5\frac{\partial^3 v}{\partial z\,\partial\tau^2} + C_2\frac{\partial^3 u}{\partial z\,\partial\tau^2} + C_4\frac{\partial u}{\partial z} + C_6\frac{\partial v}{\partial z},$$

$$P_r = P_l + C_7\left[\frac{\partial^2 u}{\partial\tau^2} - 2\gamma\frac{\partial v}{\partial\tau} - \gamma^2 u\right], \qquad Q_r = Q_l + C_7\left[\frac{\partial^2 v}{\partial\tau^2} + 2\gamma\frac{\partial u}{\partial\tau} - \gamma^2 v\right]. \tag{3}$$

In the rotating frame of reference, continuity equations of displacements and slopes at the disk point can be expressed by

$$u_r = u_l, \qquad v_r = v_l, \qquad \alpha_r = \alpha_l, \qquad \beta_r = \beta_l. \tag{4}$$

2.2. SHAFT

Consider a flexible non-axisymmetrical Rayleigh shaft including the effects of the gyroscopic moment and rotary inertia. In a rotating frame of reference, the equations of motion, as also shown in Kang *et al*. [13], are expressed by

$$\Psi_v \frac{\partial^4 U}{\partial Z^4} - \frac{\rho \Psi_v}{E} \frac{\partial^4 U}{\partial Z^2 \, \partial t^2} - \frac{\rho \Psi_v \Omega^2}{E} \frac{\partial^2 U}{\partial Z^2} + \frac{\rho A}{E} \left(\frac{\partial^2 U}{\partial t^2} - 2\Omega \frac{\partial V}{\partial t} - \Omega^2 U \right) = 0 \tag{5a}$$

in the U–Z plane, and

$$\Psi_u \frac{\partial^4 V}{\partial Z^4} - \frac{\rho \Psi_u}{E} \frac{\partial^4 V}{\partial Z^2 \, \partial t^2} - \frac{\rho \Psi_u \Omega^2}{E} \frac{\partial^2 V}{\partial Z^2} + \frac{\rho A}{E} \left(\frac{\partial^2 V}{\partial t^2} + 2\Omega \frac{\partial U}{\partial t} - \Omega^2 V \right) = 0 \tag{5b}$$

in the V–Z plane. Using non-dimensional quantities, equations (5a) and (5b) become

$$\varepsilon_v \left(\frac{\partial^4 u}{\partial z^4} - a \frac{\partial^4 u}{\partial z^2 \, \partial \tau^2} \right) - \gamma^2 \varepsilon_v a \frac{\partial^2 u}{\partial z^2} + ab \left(\frac{\partial^2 u}{\partial \tau^2} - 2\gamma \frac{\partial v}{\partial \tau} - \gamma^2 u \right) = 0 \tag{6a}$$

and

$$\varepsilon_u \left(\frac{\partial^4 v}{\partial z^4} - a \frac{\partial^4 v}{\partial z^2 \, \partial \tau^2} \right) - \gamma^2 \varepsilon_u a \frac{\partial^2 v}{\partial z^2} + ab \left(\frac{\partial^2 v}{\partial \tau^2} + 2\gamma \frac{\partial u}{\partial \tau} - \gamma^2 v \right) = 0, \tag{6b}$$

where $\varepsilon_v = \Psi_v/\Psi$, $\varepsilon_u = \Psi_u/\Psi$, $2\Psi = (\Psi_u + \Psi_v)$, $a = \rho\Omega_0^2 L^2/E$ and $b = AL^2/\Psi$.

2.3. BEARINGS

A linear bearing which is considered to be decoupled between the translational and rotational displacements can be modelled by eight coefficients, i.e., two direct stiffness coefficients K_{xx} and K_{yy}, two cross-stiffness coefficients K_{xy} and K_{yx}, two direct damping coefficients C_{xx} and C_{yy}, and two cross-damping coefficients C_{xy} and C_{yx}. In the fixed frame of reference, the equilibrium equations at the bearing point, as shown in Figure 3, are

$$\mathscr{P}'_r = \mathscr{P}'_l - K_{xx} X_l - K_{xy} Y_l - C_{xx} \dot{X}_l - C_{xy} \dot{Y}_l$$

in the X–Z plane, and

$$\mathscr{Q}'_r = \mathscr{Q}'_l - K_{yy} Y_l - K_{yx} X_l - C_{yy} \dot{Y}_l - C_{yx} \dot{X}_l \tag{7}$$

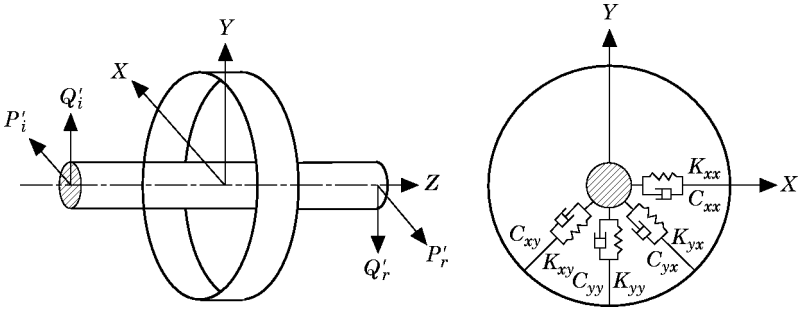

Figure 3. The force components of a bearing model.

in the Y–Z plane. Using co-ordinate transformation, the equilibrium equations in the rotating frame of reference can be expressed by non-dimensional quantities, as follows:

$$\begin{aligned}
P_r = P_l &- ((k_{xx} + \gamma\zeta_{xy})(1 + \cos 2\gamma\tau)/2 + (k_{xy} + k_{yx} + \gamma\zeta_{yy} - \gamma\zeta_{xx})(\sin 2\gamma\tau/2) \\
&+ (k_{yy} - \gamma\zeta_{yx})(1 - \cos 2\gamma\tau)/2)u_l + ((-k_{xy} + \gamma\zeta_{xx})(1 + \cos 2\gamma\tau)/2 + (-k_{yy} + k_{xx} \\
&+ \gamma\zeta_{xy} + \gamma\zeta_{yx})(\sin 2\gamma\tau/2) + (k_{yx} + \gamma\zeta_{yy})(1 - \cos 2\gamma\tau)/2)v_l - (\zeta_{xx}(1 + \cos 2\gamma\tau)/2 \\
&+ (\zeta_{xy} + \zeta_{yx})(\sin 2\gamma\tau/2) + \zeta_{yy}(1 - \cos 2\gamma\tau)/2)\dot{u}_l - (\zeta_{xy}(1 + \cos 2\gamma\tau)/2 \\
&+ (\zeta_{yy} - \zeta_{xx})(\sin 2\gamma\tau/2) - \zeta_{yx}(1 - \cos 2\gamma\tau)/2)\dot{v}_l, \\
Q_r = Q_l &- ((k_{xy} + \gamma\zeta_{yy})(1 + \cos 2\gamma\tau)/2 - (k_{xx} - k_{yy} + \gamma\zeta_{xy} + \gamma\zeta_{yx})(\sin 2\gamma\tau/2) \\
&- (k_{xy} - \gamma\zeta_{xx})(1 - \cos 2\gamma\tau)/2)u_l + ((-k_{yy} + \gamma\zeta_{yx})(1 + \cos 2\gamma\tau)/2 + (k_{xy} + k_{yx} \\
&+ \gamma\zeta_{yy} - \gamma\zeta_{xx})(\sin 2\gamma\tau/2) - (k_{xx} + \gamma\zeta_{xy})(1 - \cos 2\gamma\tau)/2)v_l - (\zeta_{yx}(1 + \cos 2\gamma\tau)/2 \\
&+ (\zeta_{yy} - \zeta_{xx})(\sin 2\gamma\tau/2) - \zeta_{xy}(1 - \cos 2\gamma\tau)/2)\dot{u}_l - (\zeta_{yy}(1 + \cos 2\gamma\tau)/2 \\
&- (\zeta_{yx} + \zeta_{xy})(\sin 2\gamma\tau/2) + \zeta_{xx}(1 - \cos 2\gamma\tau)/2)\dot{v}_l, \qquad (8a)
\end{aligned}$$

where $k_{ij} = K_{ij}L^3/(E\Psi)$ and $\zeta_{ij} = C_{ij}\Omega_0 L^3/(E\Psi)$. Periodically varying coefficients appear in the above equations. Additionally, the compatibility and moment equilibrium equations at a bearing are

$$u_r = u_l, \qquad \alpha_r = \alpha_l, \qquad M_r = M_l, \qquad v_r = v_l, \qquad \beta_r = \beta_l, \qquad N_r = N_l. \qquad (8b)$$

3. TRANSITION CURVES OF INSTABILITY

The governing equations of a non-axisymmetrical shaft and a non-axisymmetrical disk in a rotating frame of reference have constant coefficients. When the bearings are axisymmetrical, the exact solutions in free vibration can be obtained by solving simultaneous equations with constant coefficients. However, if a bearing is non-axisymmetrical, periodically varying coefficients appear in the governing equations in the rotating frame. Only approximate solutions instead of closed form solutions can be obtained.

Bolotin [4] demonstrated that, according to the Floquet theory, the problem of finding the unstable regions is reduced to the determination of the transition curves under which the free motion has a periodic solution with periods T and $2T$ ($T = 2\pi/\omega$). A direct approach is to substitute the appropriate periodic series into the equations of motion, and approximate solutions are obtained from the truncated Hill's determinant.

Since the governing equations in the rotating frame of reference have time-varying coefficients with a frequency of double the speed, the transition curves of the T-type and $2T$-type motions are

$$f_T(t) = \sum_{n=0,1,2,\ldots}^{\infty} (f_{cn}\cos 2n\gamma\tau + f_{sn}\sin 2n\gamma\tau) = \sum_{n=0,2,4,\ldots}^{\infty} (f_{cn}\cos n\gamma\tau + f_{sn}\sin n\gamma\tau) \qquad (9a)$$

with period π/γ $(=2\pi/2\gamma)$, and

$$f_{2T}(t) = \sum_{n=1,2,3,\ldots}^{\infty} \left(f_{cn} \cos\left(\frac{2n-1}{2} 2\gamma\tau\right) + f_{sn} \sin\left(\frac{2n-1}{2} 2\gamma\tau\right)\right)$$

$$= \sum_{n=1,3,5\ldots}^{\infty} (f_{cn} \cos n\gamma\tau + f_{sn} \sin n\gamma\tau) \tag{9b}$$

with the period $2\pi/\gamma$, respectively, where f is utilized to denote all of the state variables u, v, α, β, P, Q, M and N.

T-type solutions include $1\times, 3\times, \ldots$ $(n = 0, 2, \ldots)$ and other odd order harmonic motions of the free whirl. On the other hand, $2T$-type solutions include $2\times, 4\times, \ldots$ $(n = 1, 3, \ldots)$ and other even order harmonic motions of the free whirl. The complete motions can be expressed by combining equations (9a) and (9b) as follows:

$$f(t) = \sum_{n=0,1,2,\ldots}^{\infty} (f_{cn} \cos n\gamma\tau + f_{sn} \sin n\gamma\tau). \tag{9c}$$

Substituting equation (9c) into the equations of motion, the transfer matrices can be obtained by constructing the relationships of the state variables between both sides of the components.

4. FORMULATION OF TRANSFER MATRIX

4.1. DISK

Substituting equation (9c) into equations (3) and (4), and equating the coefficients in the same harmonic terms, gives

$$\begin{gathered}
(u_0)_v = (u_0)_l, \qquad (v_0)_r = (v_0)_l, \qquad (\alpha_0)_r = (\alpha_0)_l, \qquad (\beta_0)_r = (\beta_0)_l, \\
(P_0)_r = (P_0 - C_7\gamma^2 u_0)_l, \qquad (Q_0)_r = (Q_0 - C_7\gamma^2 v_0)_l, \\
(M_0)_r = (M_0 + C_3\alpha_0 + C_4\beta_0)_l, \qquad (N_0)_r = (N_0 + C_6\beta_0 + C_4\alpha_0)_l
\end{gathered} \tag{10a}$$

for the zeroth order, and

$$\begin{gathered}
(u_{sn})_r = (u_{sn})_l, \qquad (u_{cn})_r = (u_{cn})_l, \qquad (\alpha_{sn})_r = (\alpha_{sn})_l, \qquad (\alpha_{cn})_r = (\alpha_{cn})_l, \\
(v_{sn})_r = (v_{sn})_l, \qquad (v_{cn})_r = (v_{cn})_l, \qquad (\beta_{sn})_r = (\beta_{sn})_l, \qquad (\beta_{cn})_r = (\beta_{cn})_l, \\
(P_{sn})_r = (P_{sn} - C_7\gamma^2(n^2+1)u_{sn} - 2n\gamma^2 C_7 v_{cn})_l, \\
(P_{cn})_r = (P_{cn} - C_7\gamma^2(n^2+1)u_{cn} - 2n\gamma^2 C_7 v_{sn})_l, \\
(Q_{sn})_r = (Q_{sn} - C_7\gamma^2(n^2+1)v_{sn} - 2n\gamma^2 C_7 u_{cn})_l, \\
(Q_{cn})_r = (Q_{cn} - C_7\gamma^2(n^2+1)v_{cn} - 2n\gamma^2 C_7 u_{sn})_l, \\
(M_{sn})_r = (M_{sn} + (-n^2\gamma^2 C_1 + C_3)\alpha_{sn} + (-n^2\gamma^2 C_2 + C_4)\beta_{sn})_l, \\
(M_{cn})_r = (M_{cn} + (-n^2\gamma^2 C_1 + C_3)\alpha_{cn} + (-n^2\gamma^2 C_2 + C_4)\beta_{cn})_l, \\
(N_{sn})_r = (N_{sn} + (-n^2\gamma^2 C_5 + C_6)\beta_{sn} + (-n^2\gamma^2 C_2 + C_4)\alpha_{sn})_l, \\
(N_{cn})_r = (N_{cn} + (-n^2\gamma^2 C_5 + C_6)\beta_{cn} + (-n^2\gamma^2 C_2 + C_4)\alpha_{cn})_l,
\end{gathered} \tag{10b}$$

for the nth order, where $n = 1, 2, 3, \ldots, \infty$ and $C_1, C_2, \ldots, C_7$ are defined in equation (3). The transfer matrix of a non-axisymmetrical disk is constructed by assembling equations (10a) and (10b) into a matrix form as

$$\{\mathbf{S}_0\}_r = [\mathbf{T}_0^d]_{8\times 8}\{\mathbf{S}_0\}_l \tag{11a}$$

for the zeroth order, and

$$\{\mathbf{S}_n\}_r = [\mathbf{T}_n^d]_{16\times 16}\{\mathbf{S}_n\}_l \tag{11b}$$

for the nth order, where $\{\mathbf{S}_0\} = (u_0, v_0, \alpha_0, \beta_0, M_0, N_0, P_0, Q_0)^{\mathrm{T}}$ and $\{\mathbf{S}_n\} = (u_{cn}, u_{sn}, v_{cn}, v_{sn}, \alpha_{cn}, \alpha_{sn}, \beta_{cn}, \beta_{sn}, M_{cn}, M_{sn}, N_{cn}, N_{sn}, P_{cn}, P_{sn}, Q_{cn}, Q_{sn})^{\mathrm{T}}$ are state vectors.

4.2. SHAFT

Where the free vibration at the transition curves is concerned, the homogeneous solutions of equations (6a) and (6b) can be assumed by

$$u = \sum_{n=0}^{\infty} (U_{cn}\cos n\gamma\tau + U_{sn}\sin n\gamma\tau)\,\mathrm{e}^{\sigma_n z},$$

$$v = \sum_{n=0}^{\infty} (V_{cn}\cos n\gamma\tau + V_{sn}\sin n\gamma\tau)\,\mathrm{e}^{\sigma_n z}. \tag{12}$$

Evidently, the non-dimensional frequency of the free whirl in the stationary frame is $(n+1)\gamma$ given by equation (12). Substituting equation (12) into equation (6a) and (6b), the eigenvalues σ_n and the eigenfunctions U_{cn}, U_{sn}, V_{cn} and V_{sn} are determined. A general solution of the free whirl at the instability boundaries is then given by

$$u = u_0 + \sum_{n=1}^{\infty} u_n = \{f_0\}^{\mathrm{T}}\{w_0^*\} + \sum_{n=1}^{\infty} (\{f_{cn}\}^{\mathrm{T}}\{w_n^*\}\cos n\gamma\tau + \{f_{sn}\}^{\mathrm{T}}\{w_n\}\sin n\gamma\tau),$$

$$v = v_0 + \sum_{n=1}^{\infty} v_n = \{g_0\}^{\mathrm{T}}\{w_0\} + \sum_{n=1}^{\infty} (\{g_{cn}\}^{\mathrm{T}}\{w_n\}\cos n\gamma\tau + \{g_{sn}\}^{\mathrm{T}}\{w_{\mathrm{n}}^*\}\sin n\gamma\tau), \tag{13}$$

where $\{w\}$ and $\{w^*\}$ are the vectors of the real constant coefficients, and $\{f\}$ and $\{g\}$ are the vectors of the shape function. The details of the derivation of equation (13) are provided in Appendix A.

Due to the above approach, the shape functions provided by this study are exact ones. However, on the basis of finite element methods, the shape functions utilized in the consistent approach are assumed by the polynomial forms and the accuracy of the solutions is dependent on the order of these polynomials. Theoretically, a polynomial of infinite order corresponds to the exact solution, but in practice polynomials of finite order are used as an approximation. The transfer matrix derived from the conventional approach is constructed by assuming that the total masses are taken lumped at discrete stations and are connected by massless flexible elements. The accuracy of both the finite element and the conventional transfer matrix approaches can be improved by increasing the partitioned number of the shaft. However, the smallest number of shaft segments is required in the approach used in this study.

Equation (13) can be rewritten into a matrix form for formulating the relationship between the shape functions and the real constant coefficients, as follows:

$$\underset{8\times 1}{\{\mathfrak{R}_0(z)\}} = \underset{8\times 1}{\begin{bmatrix}\{\mathbf{u}_0(z)\}\\ \{\mathbf{v}_0(z)\}\end{bmatrix}} = \underset{8\times 8}{[M_0(z)]}\underset{8\times 1}{\begin{bmatrix}w_1\\ \vdots\\ w_8\end{bmatrix}} = \underset{8\times 8}{[M_0(z)]}\underset{8\times 1}{\{W_0\}} \tag{14a}$$

for the zeroth order, and

$$\underset{16\times 1}{\{\mathfrak{R}_n(z)\}} = \begin{bmatrix}\{\mathbf{u}_{sn}(z)\}\\ \{\mathbf{u}_{cn}(z)\}\\ \{\mathbf{v}_{sn}(z)\}\\ \{\mathbf{v}_{sn}(z)\}\end{bmatrix} = \underset{16\times 16}{[M_n(z)]}\begin{bmatrix}w_1\\ w_2\\ \vdots\\ w_{16}\end{bmatrix} = \underset{16\times 16}{[M_n(z)]}\underset{16\times 1}{\{W_n\}} \tag{14b}$$

for the nth order, where

$$\{\mathbf{u}_0\} = \left[u_0\ \frac{\partial u_0}{\partial z}\ \frac{\partial^2 u_0}{\partial z^2}\ \frac{\partial^3 u_0}{\partial z^3}\right]^{\mathrm{T}}, \qquad \{W_0\} = (\{w_0\}^{\mathrm{T}}\{w_0^*\}^{\mathrm{T}})^{\mathrm{T}}, \qquad \{W_n\} = (\{w_n\}^{\mathrm{T}}\{w_n^*\}^{\mathrm{T}})^{\mathrm{T}}$$

and $\{\mathbf{v}_0\}$, $\{\mathbf{u}_{cn}\}$, $\{\mathbf{u}_{sn}\}$, $\{\mathbf{v}_{cn}\}$ and $\{\mathbf{v}_{sn}\}$ have similar forms. At both ends, $z = 0$ and $z = 1$, of an uniformly non-axisymmetrical shaft, equation (14a) becomes

$$\{\mathfrak{R}_0(z=0)\} = [M_0(0)]\{W_0\}, \qquad \{\mathfrak{R}_0(z=1)\} = [M_0(1)]\{W_0\} \tag{15a, b}$$

respectively. Combining equations (15a) and (15b) gives

$$\{\mathfrak{R}_0(z=1)\} = [M_0(1)][M_0(0)]^{-1}\{\mathfrak{R}_0(z=0)\}. \tag{16a}$$

Similarly,

$$\{\mathfrak{R}_n(z=1)\} = [M_n(1)][M_n(0)]^{-1}\{\mathfrak{R}_n(z=0)\}. \tag{16b}$$

The relationships between the state variables and the derivatives of the deflections are obtained from the equations of compatibility and elastic relationships as shown by

$$\underset{8\times 8}{[\Gamma_0]}\{\mathfrak{R}_0\}, \qquad \{\mathbf{S}_n\} = \underset{16\times 16}{[\Gamma_n]}\{\mathfrak{R}_n\}, \tag{17a, b}$$

where $[\Gamma_0]$ and $[\Gamma_n]$ are shown in Appendix B. Substituting equation (16a) into equation (17a) gives

$$\{\mathbf{S}_0\}_{z=1} = [\Gamma_0][M_0(1)][M_0(0)]^{-1}[\Gamma_0]^{-1}\{\mathbf{S}_0\}_{z=0} = [\mathbf{T}_0^s]\{\mathbf{S}_0\}_{z=0}. \tag{18a}$$

Similarly,

$$\{\mathbf{S}_n\}_{z=1} = [\Gamma_n][M_n(1)][M_n(0)]^{-1}[\Gamma_n]^{-1}\{\mathbf{S}_n\}_{z=0} = [\mathbf{T}_n^s]\{\mathbf{S}_n\}_{z=0}. \tag{18b}$$

Consequently, the transfer matrices $[\mathbf{T}_0^s]$ and $[\mathbf{T}_n^s]$ in a non-axisymmetrical shaft segment are obtained in the rotating frame of reference. This approach uses continuous-system sense to formulate the transfer matrix of the shaft. Infinite modes of resonance are considered in the formulation.

4.3. BEARINGS

Substituting equation (9c) into equation (8a) gives

$$\{\mathbf{q}\}_r = [\Phi]\begin{bmatrix}\{\mathbf{x}\}\\ \{\mathbf{q}\}\end{bmatrix}_l, \tag{19}$$

where

$$\{\mathbf{x}\} = (u_0 \quad v_0 \quad u_{c1} \quad u_{s1} \quad v_{c1} \quad v_{s1} \quad \dots \quad u_{cn} \quad u_{sn} \quad v_{cn} \quad v_{sn} \quad \dots)^{\mathrm{T}}$$

and

$$\{\mathbf{q}\} = (P_0 \quad Q_0 \quad P_{c1} \quad P_{s1} \quad Q_{c1} \quad Q_{s1} \quad \dots \quad P_{cn} \quad P_{sn} \quad Q_{cn} \quad Q_{sn} \quad \dots)^{\mathrm{T}}.$$

Substituting the form of u, v, α, β, M and N in equation (9c) into equation (8b), and combining with equation (19), gives the transfer matrix of a bearing as

$$\begin{bmatrix}\{\mathbf{S}_0\}\\ \{\mathbf{S}_1\}\\ \{\mathbf{S}_2\}\\ \{\mathbf{S}_3\}\\ \{\mathbf{S}_4\}\\ \vdots\\ \vdots\\ \vdots\end{bmatrix}_r = [\mathbf{T}^b]\begin{bmatrix}\{\mathbf{S}_0\}\\ \{\mathbf{S}_1\}\\ \{\mathbf{S}_2\}\\ \{\mathbf{S}_3\}\\ \{\mathbf{S}_4\}\\ \vdots\\ \vdots\\ \vdots\end{bmatrix}_l = \begin{bmatrix} T^b_{20} & 0 & T^b_{32} & 0 & 0 & 0 & 0 & \cdots\\ 0 & T^b_{21} & 0 & T^b_{33} & 0 & 0 & 0 & \cdots\\ T^b_{10} & 0 & T^b_{22} & 0 & T^b_{34} & 0 & 0 & \cdots\\ 0 & T^b_{11} & 0 & T^b_{23} & 0 & T^b_{35} & 0 & \cdots\\ 0 & 0 & T^b_{12} & 0 & T^b_{24} & 0 & T^b_{36} & \cdots\\ 0 & 0 & 0 & T^b_{13} & 0 & T^b_{25} & 0 & \cdots\\ 0 & 0 & 0 & 0 & T^b_{14} & 0 & \ddots & \cdots\\ \cdots & \cdots & \cdots & \cdots & \cdots & \cdots & \cdots & \cdots \end{bmatrix}\begin{bmatrix}\{\mathbf{S}_0\}\\ \{\mathbf{S}_1\}\\ \{\mathbf{S}_2\}\\ \{\mathbf{S}_3\}\\ \{\mathbf{S}_4\}\\ \vdots\\ \vdots\\ \vdots\end{bmatrix}_l, \tag{20}$$

where the first subscript of T_{ij} denotes the coefficients to be related to the harmonic functions of $(n-2)\gamma\tau$, $n\gamma\tau$ and $(n+2)\gamma\tau$ by 1, 2 and 3, respectively, and the second subscript denotes the number of the harmonic order of the free whirls.

Since the transfer matrix of the bearing contains all orders of harmonic motion, it is called the extended transfer matrix. At the same time, the extended state vector includes state variables of all the harmonic orders.

When the bearing or the stator are axisymmetrical, the coefficients T_{1n} and T_{3n} vanish, and the state vectors among all orders of the bearing are decoupled; then the transfer matrix has the same form as the shaft or the disk.

It is also noticed that only two state vectors $\{\mathbf{S}_{n-2}\}$ and $\{\mathbf{S}_{n+2}\}$ are correlated by $\{\mathbf{S}_n\}$. Therefore, equation (20) can be divided into

$$\{\mathbf{S}_T\}_r = \begin{bmatrix}\{\mathbf{S}_0\}\\ \{\mathbf{S}_2\}\\ \{\mathbf{S}_4\}\\ \vdots\\ \vdots\end{bmatrix}_r = \begin{bmatrix} T^b_{20} & T^b_{32} & 0 & 0 & \cdots\\ T^b_{10} & T^b_{22} & T^b_{34} & 0 & \cdots\\ 0 & T^b_{12} & T^b_{24} & T^b_{36} & \cdots\\ 0 & 0 & T^b_{14} & \ddots & \cdots\\ \cdots & \cdots & \cdots & \cdots & \cdots \end{bmatrix}\begin{bmatrix}\{\mathbf{S}_0\}\\ \{\mathbf{S}_2\}\\ \{\mathbf{S}_4\}\\ \vdots\\ \vdots\end{bmatrix}_l = [\mathbf{T}^b_T]\{\mathbf{S}_T\}_l \tag{21a}$$

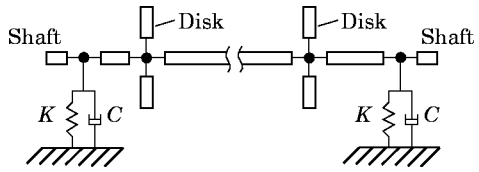

Figure 4. A general rotor–bearing system.

for the T-type motion, and

$$\{\mathbf{S}_{2T}\}_r = \begin{bmatrix} \{\mathbf{S}_1\} \\ \{\mathbf{S}_3\} \\ \{\mathbf{S}_5\} \\ \vdots \\ \vdots \end{bmatrix}_r = \begin{bmatrix} T_{21}^b & T_{33}^b & 0 & 0 & \cdots \\ T_{11}^b & T_{23}^b & T_{35}^b & 0 & \cdots \\ 0 & T_{13}^b & T_{25}^b & T_{37}^b & \cdots \\ 0 & 0 & T_{15}^b & \ddots & \cdots \\ \cdots & \cdots & \cdots & \cdots & \cdots \end{bmatrix} \begin{bmatrix} \{\mathbf{S}_1\} \\ \{\mathbf{S}_3\} \\ \{\mathbf{S}_5\} \\ \vdots \\ \vdots \end{bmatrix}_l = [\mathbf{T}_{2T}^b]\{\mathbf{S}_{2T}\}_l \tag{21b}$$

for the $2T$-type motion. In the above equations, $\{\mathbf{S}_T\}$ and $\{\mathbf{S}_{2T}\}$ are the extended state vectors including the state variables of all even and odd harmonic motions, respectively.

In a rotating frame of reference, periodic terms will appear in the equations for the bearing: however, the governing equations of non-axisymmetrical shafts have constant coefficients. Thus, it is convenient to formulate the transfer matrix of the shaft by shape functions, since these shape functions and the transfer matrix are all constant coefficients in the rotating frame.

5. SOLUTION METHOD

Since the form of the transfer matrix of the bearing is different from that of the shaft and the disk, the matrices and the state vectors of each must be modified to the same form before constructing transfer matrices of an overall rotor–bearing system. Thus, equation (11) must be changed to

$$\{\mathbf{S}_T\}_r = [\mathbf{T}_T^d]\{\mathbf{S}_T\}_l, \qquad \{\mathbf{S}_{2T}\}_r = [\mathbf{T}_{2T}^d]\{\mathbf{S}_{2T}\}_l \tag{22a, b}$$

and equations (18a) and (18b) are changed to

$$\{\mathbf{S}_T\}_r = [\mathbf{T}_T^s]\{\mathbf{S}_T\}_l, \qquad \{\mathbf{S}_{2T}\}_r = [\mathbf{T}_{2T}^s]\{\mathbf{S}_{2T}\}_l, \tag{23a, b}$$

where

$$[T_T^i] = \begin{bmatrix} T_0^i & 0 & 0 & \cdots \\ 0 & T_2^i & 0 & \cdots \\ 0 & 0 & \ddots & \cdots \\ \cdots & \cdots & \cdots & \cdots \end{bmatrix} \text{ and } [T_{2T}^i] = \begin{bmatrix} T_1^i & 0 & 0 & \cdots \\ 0 & T_3^i & 0 & \cdots \\ 0 & 0 & \ddots & \cdots \\ \cdots & \cdots & \cdots & \cdots \end{bmatrix}, \qquad i = d, s.$$

Let R and L denote the right and the left sides of the overall system, respectively. The overall transfer matrix of a system, as shown in Figure 4, is obtained by

$$\{\mathbf{S}_T\}_R = \prod_{i=N}^{1} [\mathbf{T}_T]_i \{\mathbf{S}_T\}_L = [\mathbf{T}_T^o]\{\mathbf{S}_T\}_L \tag{24a}$$

for the T-type motion, and

$$\{\mathbf{S}_{2T}\}_R = \prod_{i=N}^{1} [\mathbf{T}_{2T}]_i \{\mathbf{S}_{2T}\}_L = [\mathbf{T}^o_{2T}]\{\mathbf{S}_{2T}\}_L \tag{24b}$$

for the $2T$-type motion, where

$$\prod_{i=N}^{1} [\mathbf{T}_T]_i \text{ and } \prod_{i=N}^{1} [\mathbf{T}_{2T}]_i$$

represent the product of transfer matrices from the first station (denoted by L) to the nth station (denoted by R). Thus, the two Hill's infinite determinants of the T- and $2T$-type motions are obtained independently. The roots of the truncated determinants of $[\mathbf{T}^o_T]$ and $[\mathbf{T}^o_{2T}]$ give approximate solutions of T- and $2T$-type transition curves respectively.

Based on the boundary conditions of the rotor–bearing system being satisfied, equations (24a) and (24b) are formulated as

$$\begin{bmatrix} \{\mathbf{\Phi}\} \\ \{\mathbf{0}\} \end{bmatrix}_R = \begin{bmatrix} \mathbf{T}_1 & \mathbf{T}_2 \\ \mathbf{T}_3 & \mathbf{T}_4 \end{bmatrix} \begin{bmatrix} \{\mathbf{\Phi}\} \\ \{\mathbf{0}\} \end{bmatrix}_L, \tag{25}$$

where $\{\mathbf{0}\}$ is the zero state vector, and $\{\mathbf{\Phi}\}_R$ and $\{\mathbf{\Phi}\}_L$ are formed by non-zero state variables, at both ends of a rotor–bearing system. For example, when the shear forces and bending moments are free at both ends and n harmonic terms of equation (9c) are considered, $\{\mathbf{\Phi}\}_R$, $\{\mathbf{\Phi}\}_L = (u_0\ v_0\ \alpha_0\ \beta_0\ u_{c2}\ u_{s2}\ v_{c2}\ v_{s2}\ \alpha_{c2}\ \alpha_{s2}\ \beta_{c2}\ \beta_{s2}\ \ldots\ u_{cn}\ \ldots\ \beta_{sn})^{\mathrm{T}}$, both vectors have dimensions of $4n + 4$, and $\{\mathbf{0}\}$ is a zero vector with dimensions $4n + 4$. For the non-trivial solution of $\{\mathbf{\Phi}\}$, one has

$$|\mathbf{T}_3(\gamma)| = 0. \tag{26}$$

Equation (26), derived from equation (24a), gives T-type solutions and the one derived from equation (24b) gives $2T$-type solutions. Unstable regions of synchronous and subcritical modes with odd multiple speeds are bounded by transition curves of the T-type solutions. On the other hand, unstable regions of subcritical modes with even multiple speeds are bounded by transition curves of the $2T$-type solutions.

6. NUMERICAL EXAMPLES

A model of a uniform non-axisymmetrical shaft was utilized to verify the formulation and the algorithm for instability analysis. The physical parameters of this shaft are $L = 2\,\mathrm{m}$, $E = 2 \times 10^{11}\,\mathrm{N/m^2}$, $A = 7{\cdot}85 \times 10^{-3}\,\mathrm{m^2}$, $\rho = 7750\,\mathrm{kg/m^3}$, and the stiffness and damping coefficients of the bearing are assumed to be constant in the speed range under consideration.

When bearings are axisymmetrical, the coefficients are assumed to be $C_{ij} = 0$, $K_{xx} = K_{yy} = k\pi^4(E\Psi/L^3)$ and $K_{xy} = K_{yx} = 0$. The unstable regions due to various values of non-dimensional factor k are shown in Figure 5. Solid curves and dashed curves are utilized to illustrate the transition curves of instability belonging to T-type and $2T$-type solutions respectively. The T-type solution of free motion contains only the main modes of synchronous whirl, denoted by $1\times$. The $2T$-type solution contains subcritical modes of double-speed whirl, denoted by $2\times$. The first subscript of P_{ij} denotes the unstable region belonging to the ith main mode, and the second subscript denotes the rigid body motion or the flexural mode.

When $k = 0{\cdot}01$, the stiffness of the bearing is much smaller than that of the shaft. Therefore, the first two modes of the rigid body motion are very slightly affected by the asymmetry of the shaft. When $k = 0{\cdot}1$, the unstable regions of the rigid body motions expand, but the size is still smaller than that in the flexural mode. When $k = 1$ the stiffness of the bearing and the shaft almost equal, both rigid body motions vanish and all unstable regions belong to the flexural mode. As k increases to 100, the plot of the low modes is closely similar to that of the same shaft with the boundary conditions of both hinged–hinged ends.

When Δ/Ψ is increasing, the unstable regions of the main modes enlarge and the subcritical speeds decrease. Due to the fact that the shaft and disk asymmetry are multiplied by the square of the rotating speeds, as shown in equations (1) and (5), the unstable region of a higher flexural mode is larger than that of a lower flexural mode. It is noticed that the support flexibility can shrink the unstable regions of all modes and reduce the speeds of the transition curves. However, instability cannot be eliminated by increasing k.

Consider the same non-axisymmetrical shaft with both non-axisymmetrical bearings which have $C_{ij} = 0$, $K_{xx} = 0{\cdot}5k\pi^4(E\Psi/L^3)$ and $K_{yy} = 1{\cdot}5k\pi^4(E\Psi/L^3)$. The T- and $2T$-type

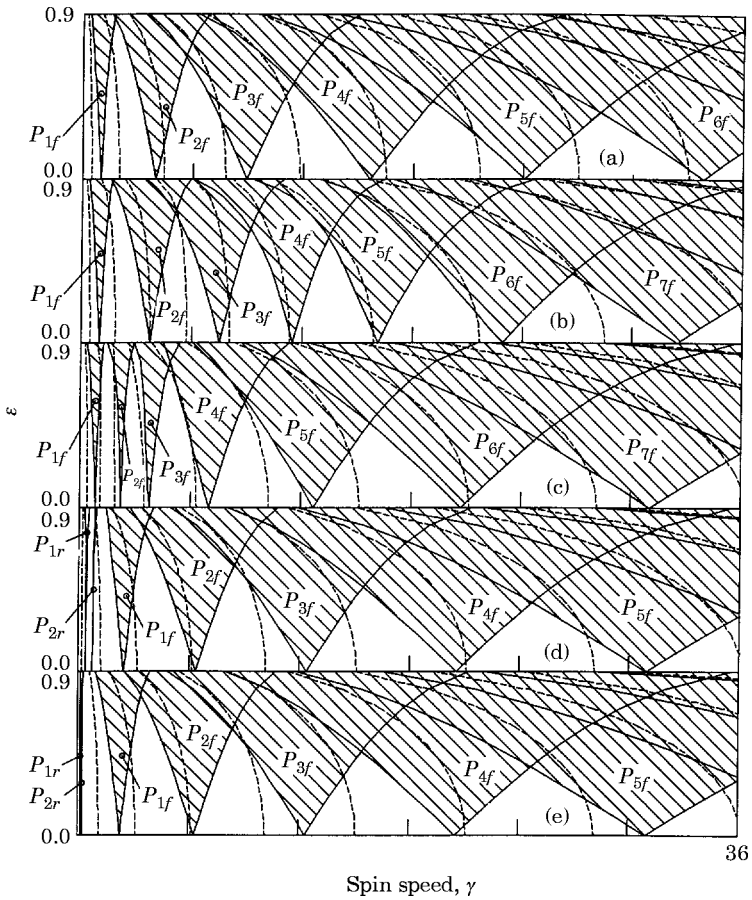

Figure 5. The unstable regions of a non-axisymmetrical shaft with a varying stiffness ($k_{xx} = k_{yy} = k\pi^4(E\Psi/L^3)$, $\zeta = 0$). (a) $k = 100$; (b) $k = 10$; (c) $k = 1$; (d) $k = 0{\cdot}1$; (e) $k = 0{\cdot}01$. ——, T-type solution; – – – –, $2T$-type solution.

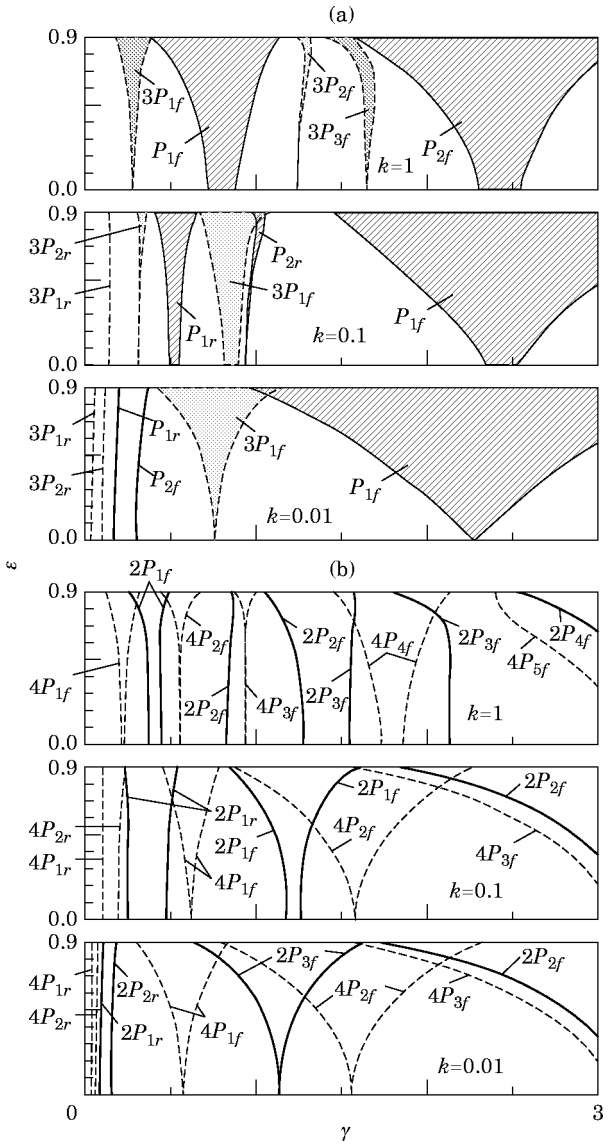

Figure 6. Transition curves and unstable regions of (a) T-type solution (the fourth order approximation; —— $1\times$ whirl, —— $3\times$ whirl) and (b) $2T$-type solution (the fifth order approximation; —— $2\times$ whirl, – – – – $4\times$ whirl).

solutions are shown in Figure 6. These curves of the $n\times$ whirl are located at about $1/n$ times the speed values of the unstable regions of the main modes. Unstable regions of the synchronous ($1\times$) whirl and the $3\times$ whirl are shown in Figure 6(a), and subcritical speeds of $2\times$ and $4\times$ whirls are shown in Figure 6(b). The number preceding P_{ij} denotes the order of subcritical resonance due to the free whirl, which has a frequency of the multiple number of the spin speed.

In the determination of the truncated T-type determinant, the zero values are obtained to give approximate transition curves of the odd $n\times$ whirls. Thus, unstable regions of the synchronous whirl and the $3\times$ whirl are obtained while, in the determination of the truncated $2T$-type determinants, the minimum values are obtained to give approximate

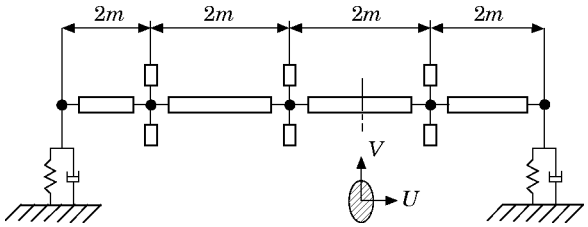

Figure 7. A model of an unsymmetrical rotor–bearing system.

subcritical speeds of the even $n\times$ whirls. Thus, the result is that there is no unstable region of subcritical resonances of even $n\times$ whirls, and subcritical speeds of $2T$-type motions reveal that there are response peaks in the free whirl which can be excited at the even $n\times$ subcritical modes. It is also shown that subcritical speeds of the $4\times$ whirl are located at about half the values of the $2\times$ whirls.

A complex rotor–bearing system shown in Figure 7, having a non-axisymmetrical shaft ($\varepsilon = \Delta/\Psi = 0{\cdot}5$) and three axisymmetrical disks, is considered. Two non-dimensional parameters $\mu_1 = I^d/(\rho\Psi A)$ and $\mu_2 = m^d/(\rho AL)$, are utilized for the moment of inertia and the mass of these identical disks. The coefficients of both axisymmetrical bearings are assumed to be $k_{xx} = k_{yy} = k$ and $\zeta_{xx} = \zeta_{yy} = \zeta$, and the other coefficients are zero.

When the parameters are $k = 10$, $\mu_1 = 14{\cdot}62$ and $\mu_2 = 7{\cdot}31$, the dependence of the shaft asymmetry on unstable regions for various damping coefficients is shown in Figure 8.

These unstable regions due to slight asymmetry in the shaft can be eliminated by damping of the bearings. In other words, unstable regions can be raised by increasing the damping coefficients. Moreover, unstable regions of the second and the third flexural modes are completely eliminated by large damping when $\zeta = 30$, as shown in this example.

Consider this system with $\Delta/\Psi = 0{\cdot}5$ and various inertias of disks. The dependence of the bearing damping on the stability is plotted in Figure 9, which shows that unstable regions move to the right when the damping coefficients increase. In the first case, with

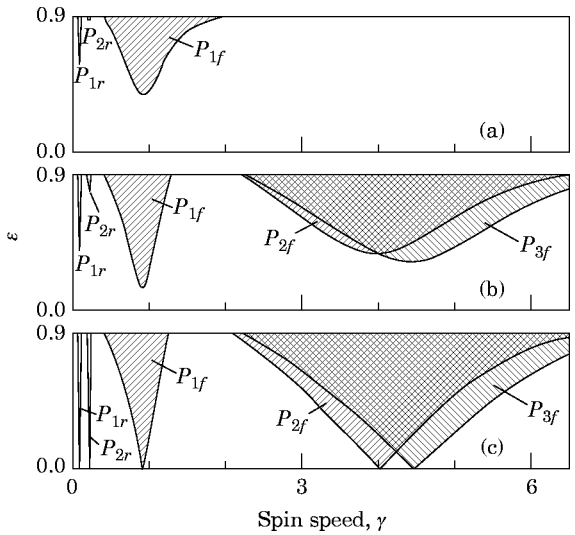

Figure 8. The influence of shaft asymmetry on unstable regions for various damping coefficients. (a) $\zeta = 30$; (b) $\zeta = 10$; (c) $\zeta = 0$.

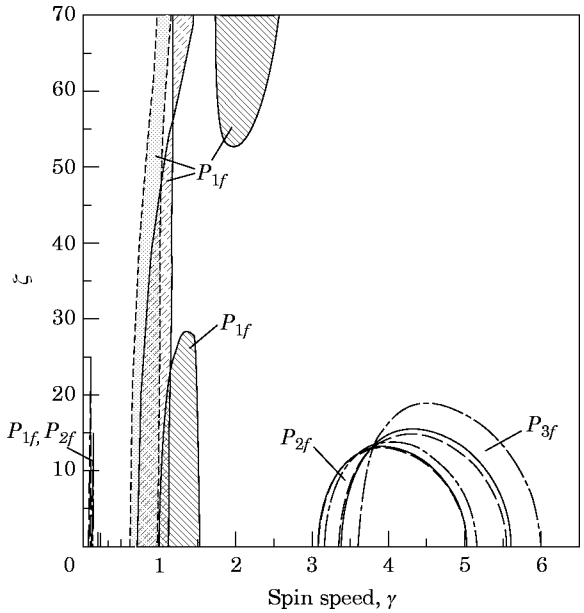

Figure 9. The influence of bearing damping on instability: $\varepsilon = 0{\cdot}5$, $k_{xx} = k_{yy} = 10$. ----, $\mu_1 = 20$, $\mu_2 = 10$; ——, $\mu_1 = 14{\cdot}62$, $\mu_2 = 7{\cdot}31$; –·–·–, $\mu_1 = 6{\cdot}67$, $\mu_2 = 3{\cdot}33$.

$\mu_1 = 20$ and $\mu_2 = 10$, there is an unstable region of about $\gamma = 1{\cdot}0$ which cannot be eliminated by changing the damping, as shown by the dashed curves. The second case, with $\mu_1 = 14{\cdot}62$ and $\mu_2 = 7{\cdot}31$ being the critical values, is shown by solid curves. When μ_1 and μ_2 are larger than the critical values, the unstable regions then cannot be eliminated by any damping coefficient. In the third case, with $\mu_1 = 6{\cdot}67$ and $\mu_2 = 3{\cdot}33$, the unstable region of the first flexural mode is eliminated from $\zeta = 28$ to $\zeta = 52$ as shown by chain curves. Also, the unstable regions of the P_{2f} and P_{3f} modes for three cases are shown by three types of transition curves without hatching. These instabilities can be completely eliminated when the damping coefficient increases to $\zeta = 15$ or $\zeta = 20$.

For the modified transfer matrix approach, the accuracy of solutions is independent on the partitioned number of shaft elements. The least number is required. For example, the system as illustrated in Figure 7 is partitioned into four elements. When either the finite element approach or the conventional transfer matrix approach is utilized, the accuracy of the solutions may be improved by increasing the partitioned number. To achieve the same accuracy, the CPU time and memory size of both approaches are much more than that of the modified transfer matrix approach. For steady state solutions, the comparisons of accuracy and CPU times between the FEM and the modified transfer matrix approach are reported by Lee *et al*. [15].

7. CONCLUSIONS

This study utilized a modified transfer matrix method to analyze the instability in unsymmetrical rotor–bearing systems. The modified transfer matrix of a shaft segment was derived from a continuous-system sense to decrease the number of matrix-multiplying operations and to achieve higher accuracy than those from a lumped-system sense. This matrix contains infinite modes, since the shape function of the shaft is derived by an

analytical method and has an exact form. Thus, one can obtain solutions for unstable regions including higher modes.

Unstable regions were obtained by determining the transition curves of the free-whirl motions of period T and period $2T$. It was shown that the unstable regions of T-type solutions are bounded by two transition curves in each mode; however, $2T$-type solutions are subcritical speeds which are minimum values of the truncated determinant. From these instability analyses, the following results can be obtained: (1) unstable regions are widened by increasing the asymmetry of the shaft in the same mode; (2) the unstable region of a higher flexural mode is larger than that of a lower flexural mode for the same shaft asymmetry; (3) the damping of the bearings has effects of stabilization and destabilization on unsymmetrical rotor–bearing systems, and the unstable regions can be eliminated by a suitable choice of system parameters.

Most commercial software packages (for example, ANSYS, COSMOS for FEM, and RAPIDD-RSR for TMM) do not have any particular element for analyzing the unsymmetrical rotor–bearing system and solving the code for a parametric instability. This study has provided these complementary contents by using the approach of the modified transfer matrix method.

REFERENCES

1. S. H. Crandall and P. J. Brosens 1961 *Journal of Applied Mechanics* **28**, 567–570. On the stability of rotation of a rotor with rotationally unsymmetric inertia and stiffness properties.
2. Y. Tamamoto and H. Ota 1964 *Journal of Applied Mechanics* **31**, 515–552. On unstable vibrations of a shaft carrying an unsymmetrical rotor.
3. D. Ardayfio and D. A. Frohrib 1976 *Journal of Engineering for Industry* **98**, 327–331. Vibration of an asymmetrically mounted rotor with gyroscopic effects.
4. C. Rajalimgham, R. B. Bhat and G. D. Xistris 1992 *International Journal of Mechanical Sciences* **34**, 717–726. Influence of support flexibility and damping characteristics on the stability of rotors with stiffness anisotropy about principal axes.
5. R. C. Arnold and E. E. Haft 1972 *Journal of Engineering for Industry* **94**, 243–249. Stability of an unsymmetrical rotating cantilever shaft carrying an unsymmetrical rotor.
6. T. Iwatsubo, H. Kawki and T. Miyaji 1980 *Bulletin of the Japan Society of Mechanical Engineers* **23**, 934–937. On the stability of a rotating asymmetric shaft supported by asymmetric bearings.
7. Y. G. Jei and C. W. Lee 1992 *Journal of Sound and Vibration* **152**, 245–262. Modal analysis of continuous asymmetrical rotor–bearing systems.
8. Y. G. Jei and C. W. Lee 1993 *Journal of Sound and Vibration* **162**, 209–229. Modal characteristics of asymmetrical rotor–bearing systems.
9. G. Genta 1988 *Journal of Sound and Vibration* **124**, 27–53. Whirling of unsymmetrical rotors: a finite element approach based on complex co-ordinates.
10. J. W. Lund 1974 *Journal of Engineering for Industry* **96**, 509–517. Stability and damped critical speeds of a flexible rotor in fluid-film bearings.
11. P. N. Bansal and R. G. Kirk 1975 *Journal of Engineering for Industry* **97**, 1325–1332. Stability and damped critical speeds of rotor–bearing systems.
12. B. T. Murphy and J. M. Vance 1983 *Journal of Engineering for Power* **103**, 591–595. An improved method for calculating critical speeds and rotordynamic stability of turbomachinery.
13. Y. Kang, A. C. Lee and Y. P. Shih 1994 *Journal of Vibration and Acoustics* **116**, 309–317. A modified transfer matrix method for asymmetric rotor bearing systems.
14. V. V. Bolotin 1964 *The Dynamic Stability of Elastic Systems*. San Francisco: Holden-Day.
15. A. C. Lee, Y. P. Shih and Y. Kang 1993 *Journal of Vibration and Acoustics* **115**, 490–497. The analysis of linear rotor-bearing systems: a general transfer matrix method.

APPENDIX A

The characteristic equation of equations (6a) and (6b) is

$$\sigma^4 + a\sigma^2(\lambda^2 - \gamma^2) = \frac{ab}{2\varepsilon_u\varepsilon_v}\left[(\varepsilon_u + \varepsilon_v)(\lambda^2 + \gamma^2) \pm (\varepsilon_u - \varepsilon_v)(\lambda^2 + \gamma^2)\right]$$

$$= \gamma_1 \text{ (of plus) and } \gamma_2 \text{ (of minus)}, \tag{A1}$$

where γ_1 and γ_2 are both postive real numbers. Related to γ_1 and γ_2, respectively, equation (A1) gives

$$\sigma^2 = \frac{-a}{2}(\lambda^2 - \gamma^2) \pm \left[\frac{a^2}{4}(\lambda^2 - \gamma^2)^2 + \gamma_1\right]^{0.5} = \gamma_3, \gamma_4$$

or

$$\sigma^2 = \frac{-a}{2}(\lambda^2 - \gamma^2) \pm \left[\frac{a^2}{4}(\lambda^2 - \gamma^2)^2 + \gamma_2\right]^{0.5} = \gamma_5, \gamma_6, \tag{A2}$$

where γ_3, γ_4, γ_5 and γ_6 are all positive real numbers. Thus the roots of equation (A1) are solved and obtained: $\sigma_{1,2} = \pm\sqrt{\gamma_3}$ and $\alpha_{5,6} = \pm\sqrt{\gamma_5}$, being real values; and $\sigma_{3,4} = \pm i\sqrt{\gamma_4}$ and $\sigma_{7,8} = \pm i\sqrt{\gamma_6}$, being pure imaginary values.

When $\lambda = 0$,

$$u_0 = w_5 \cosh\sqrt{\gamma_3}z + w_6 \sinh\sqrt{\gamma_3}z + w_7 \cos\sqrt{\gamma_4}z + w_8 \sin\sqrt{\gamma_4}z = \{f_0(z)\}^T\{w_0^*\},$$

$$v_0 = w_1 \cosh\sqrt{\gamma_5}z + w_2 \sinh\sqrt{\gamma_5}z + w_3 \cos\sqrt{\gamma_6}z + w_4 \sin\sqrt{\gamma_6}z = \{g_0(z)\}^T\{w_0\}, \tag{A3}$$

where $\{w_0\} = (w_1\ w_2\ w_3\ w_4)^T$ and $\{w_0^*\} = (w_5\ w_6\ w_7\ w_8)^T$.

When $\lambda = \gamma$,

$$u_{c1} = \frac{2ab\gamma^2}{\varepsilon_v\gamma_1 - 2ab\gamma^2}v_{s1} = \gamma_7 v_{s1}, \qquad u_{s1} = -\gamma_7 v_{c1}, \tag{A4a}$$

for $\sigma_1, \sigma_2 = \pm\sqrt{\gamma_3}$, $\sigma_3, \sigma_4 = \pm i\sqrt{\gamma_3}$ and

$$u_{c1} = v_{s1}, \qquad u_{s1} = -v_{c1}, \tag{A4b}$$

for σ_5, σ_6, σ_7, $\sigma_8 = 0$. Consequently, u and v can be expressed by

$$\begin{aligned} u_1 &= [\gamma_7(w_9 \cosh\sqrt{\gamma_3}z + w_{10} \sinh\sqrt{\gamma_3}z + w_{11} \cos\sqrt{\gamma_3}z + w_{12} \sin\sqrt{\gamma_3}z) \\ &\quad + (w_{13} + w_{14}z + w_{15}z^2 + w_{16}z^3)] \cos\gamma\tau \\ &\quad - [\gamma_7(w_1 \cosh\sqrt{\gamma_3}z + w_2 \sinh\sqrt{\gamma_3}z + w_3 \cos\sqrt{\gamma_3}z + w_4 \sin\sqrt{\gamma_3}z) \\ &\quad + (w_5 + w_6z + w_7z^2 + w_8z^3)] \sin\gamma\tau \\ &= \{f_{c1}(z)\}^T\{w_1^*\} \cos\gamma\tau + \{f_{s1}(z)\}^T\{w_1\} \sin\gamma\tau \\ &= u_{c1} \cos\gamma\tau + u_{s1} \sin\gamma\tau, \end{aligned} \tag{A5a}$$

$$\begin{aligned} v_1 &= [(w_1 \cosh\sqrt{\gamma_3}z + w_2 \sinh\sqrt{\gamma_3}z + w_3 \cos\sqrt{\gamma_3}z + w_4 \sin\sqrt{\gamma_3}z) \\ &\quad + (w_5 + w_6z + w_7z^2 + w_8z^3)] \cos\gamma\tau \\ &\quad - [(w_9 \cosh\sqrt{\gamma_3}z + w_{10} \sinh\sqrt{\gamma_3}z + w_{11} \cos\sqrt{\gamma_3}z + w_{12} \sin\sqrt{\gamma_3}z) \\ &\quad + (w_{13} + w_{14}z + w_{15}z^2 + w_{16}z^3)] \sin\gamma\tau \end{aligned}$$

$$= \{g_{c1}(z)\}^{\mathrm{T}}\{w_1\}\cos\gamma\tau + \{g_{s1}(z)\}^{\mathrm{T}}\{w_1^*\}\sin\gamma\tau$$
$$= v_{c1}\cos\gamma\tau + v_{s1}\sin\gamma\tau, \tag{A5b}$$

where $\{w_1\} = (w_1, \ldots, w_8)^{\mathrm{T}}$ and $\{w_1^*\} = (w_9, \ldots, w_{16})^{\mathrm{T}}$ are coefficient vectors of u_{c1}, u_{s1}, v_{c1} and v_{s1}.

When $\lambda \geqslant 2\gamma$,

$$u_{cn} = \frac{2ab\lambda}{\varepsilon_v\gamma_1 - ab(\lambda^2+\gamma^2)}\,v_{sn} = \gamma_8 v_{sn}, \qquad u_{sn} = -\gamma_8 v_{cn}, \tag{A6a}$$

for σ_1 to σ_4, and

$$u_{sn} = \frac{2ab\lambda}{\varepsilon_v\gamma_2 - ab(\lambda^2+\gamma^2)}\,v_{cn} = \gamma_9 v_{cn}, \qquad u_{cn} = -\gamma_9 v_{sn}, \tag{A6b}$$

for σ_5 to σ_8. Thus,

$$\begin{aligned} u_n &= [\gamma_8(w_9\cosh\sqrt{\gamma_3}z + w_{10}\sinh\sqrt{\gamma_3}z + w_{11}\cos\sqrt{\gamma_4}z + w_{12}\sin\sqrt{\gamma_4}z) \\ &\quad - \gamma_9(w_{13}\cosh\sqrt{\gamma_5}z + w_{14}\sinh\sqrt{\gamma_5}z + w_{15}\cos\sqrt{\gamma_6}z + w_{16}\sin\sqrt{\gamma_6}z)]\cos n\gamma\tau \\ &\quad - [\gamma_8(w_1\cosh\sqrt{\gamma_3}z + w_2\sinh\sqrt{\gamma_3}z + w_3\cos\sqrt{\gamma_4}z + w_4\sin\sqrt{\gamma_4}z) \\ &\quad - \gamma_9(w_5\cosh\sqrt{\gamma_5}z + w_6\sinh\sqrt{\gamma_5}z + w_7\cos\sqrt{\gamma_6}z + w_8\sin\sqrt{\gamma_6}z)]\sin n\gamma\tau \\ &= \{f_{cn}(z)\}^{\mathrm{T}}\{w_n^*\}\cos n\gamma\tau + \{f_{sn}(z)\}^{\mathrm{T}}\{w_n\}\sin n\gamma\tau \\ &= u_{cn}\cos n\gamma\tau + u_{sn}\sin n\gamma\tau, \end{aligned} \tag{A7a}$$

$$\begin{aligned} v_n &= [(w_1\cosh\sqrt{\gamma_3}z + w_2\sinh\sqrt{\gamma_3}z + w_3\cos\sqrt{\gamma_4}z + w_4\sin\sqrt{\gamma_4}z) \\ &\quad + (w_5\cosh\sqrt{\gamma_5}z + w_6\sinh\sqrt{\gamma_5}z + w_7\cos\sqrt{\gamma_6}z + w_8\sin\sqrt{\gamma_6}z)]\cos n\gamma\tau \\ &\quad + [(w_9\cosh\sqrt{\gamma_3}z + w_{10}\sinh\sqrt{\gamma_3}z + w_{11}\cos\sqrt{\gamma_4}z + w_{12}\sin\sqrt{\gamma_4}z) \\ &\quad + (w_{13}\cosh\sqrt{\gamma_5}z + w_{14}\sinh\sqrt{\gamma_5}z + w_{15}\cos\sqrt{\gamma_6}z + w_{16}\sin\sqrt{\gamma_6}z)]\sin n\gamma\tau \\ &= \{g_{cn}(z)\}^{\mathrm{T}}\{w_n\}\cos n\gamma\tau + \{g_{sn}(z)\}^{\mathrm{T}}\{w_n^*\}\sin n\gamma\tau \\ &= v_{cn}\cos n\gamma\tau + v_{sn}\sin n\gamma\tau, \end{aligned} \tag{A7b}$$

where $\{w_n\} = (w_1, \ldots, w_8)^{\mathrm{T}}$ and $\{w_n^*\} = (w_9, \ldots, w_{16})^{\mathrm{T}}$ are coefficient vectors of u_{cn}, u_{sn}, v_{cn} and v_{sn} for integer $n \geqslant 2$.

APPENDIX B

Compatible equations at both ends of a shaft are shown below:

$$\partial u/\partial z = \alpha, \qquad \partial v/\partial z = \beta, \qquad \varepsilon_v\,\partial^2 u/\partial z^2 = M, \qquad \varepsilon_u\,\partial^2 v/\partial z^2 = N,$$
$$\varepsilon_v\,\partial^3 u/\partial z^3 = P, \qquad \varepsilon_u\,\partial^3 v/\partial z^3 = Q. \tag{B1}$$

Substituting equation (13) into equation (B1) gives

$$\alpha_0 = \partial u_0/\partial z, \qquad \beta_0 = \partial v_0/\partial z, \qquad M_0 = \varepsilon_v\,\partial^2 u_0/\partial z^2, \qquad N_0 = \varepsilon_u\,\partial^2 v_0/\partial z^2,$$
$$P_0 = \varepsilon_v\,\partial^3 u_0/\partial z^3, \qquad Q_0 = \varepsilon_u\,\partial^3 v_0/\partial z^3 \tag{B2a}$$

for the zeroth order and, similarly,

$$\alpha_{cn} = \partial u_{cn}/\partial z, \qquad \beta_{cn} = \partial v_{cn}/\partial z, \qquad \alpha_{sn} = \partial u_{sn}/\partial z, \qquad \beta_{sn} = \partial v_{sn}/\partial z,$$
$$M_{cn} = \varepsilon_v\,\partial^2 u_{cn}/\partial z^2, \qquad N_{cn} = \varepsilon_u\,\partial^2 v_{cn}/\partial z^2, \qquad M_{sn} = \varepsilon_v\,\partial^2 u_{sn}/\partial z^2, \qquad N_{sn} = \varepsilon_u\,\partial^2 v_{sn}/\partial z^2,$$
$$P_{cn} = \varepsilon_v\,\partial^3 u_{cn}/\partial z^3, \qquad Q_{cn} = \varepsilon_u\,\partial^2 v_{cn}/\partial z^3, \qquad \varepsilon_v\,\partial^3 u_{sn}/\partial z^3 = P_{sn}, \qquad \varepsilon_u\partial^3 v_{sn}/\partial z^3 = Q_{sn} \tag{B2b}$$

for the nth order. Assembling equations (B2a) and (B2b) gives

$$[\Gamma_0] = \begin{bmatrix} 1 & 0 & 0 & 0 & 0 & 0 & 0 & 0 \\ 0 & 1 & 0 & 0 & 0 & 0 & 0 & 0 \\ 0 & 0 & 1 & 0 & 0 & 0 & 0 & 0 \\ 0 & 0 & 0 & 1 & 0 & 0 & 0 & 0 \\ 0 & 0 & 0 & 0 & \varepsilon_v & 0 & 0 & 0 \\ 0 & 0 & 0 & 0 & 0 & \varepsilon_u & 0 & 0 \\ 0 & 0 & 0 & 0 & 0 & 0 & \varepsilon_v & 0 \\ 0 & 0 & 0 & 0 & 0 & 0 & 0 & \varepsilon_u \end{bmatrix}$$

and

$$[\Gamma_n] = \begin{bmatrix} 1 & 0 & 0 & 0 & 0 & 0 & 0 & 0 & 0 & 0 & 0 & 0 & 0 & 0 & 0 & 0 \\ 0 & 1 & 0 & 0 & 0 & 0 & 0 & 0 & 0 & 0 & 0 & 0 & 0 & 0 & 0 & 0 \\ 0 & 0 & 1 & 0 & 0 & 0 & 0 & 0 & 0 & 0 & 0 & 0 & 0 & 0 & 0 & 0 \\ 0 & 0 & 0 & 1 & 0 & 0 & 0 & 0 & 0 & 0 & 0 & 0 & 0 & 0 & 0 & 0 \\ 0 & 0 & 0 & 0 & 1 & 0 & 0 & 0 & 0 & 0 & 0 & 0 & 0 & 0 & 0 & 0 \\ 0 & 0 & 0 & 0 & 0 & 1 & 0 & 0 & 0 & 0 & 0 & 0 & 0 & 0 & 0 & 0 \\ 0 & 0 & 0 & 0 & 0 & 0 & 1 & 0 & 0 & 0 & 0 & 0 & 0 & 0 & 0 & 0 \\ 0 & 0 & 0 & 0 & 0 & 0 & 0 & 1 & 0 & 0 & 0 & 0 & 0 & 0 & 0 & 0 \\ 0 & 0 & 0 & 0 & 0 & 0 & 0 & 0 & \varepsilon_v & 0 & 0 & 0 & 0 & 0 & 0 & 0 \\ 0 & 0 & 0 & 0 & 0 & 0 & 0 & 0 & 0 & \varepsilon_v & 0 & 0 & 0 & 0 & 0 & 0 \\ 0 & 0 & 0 & 0 & 0 & 0 & 0 & 0 & 0 & 0 & \varepsilon_u & 0 & 0 & 0 & 0 & 0 \\ 0 & 0 & 0 & 0 & 0 & 0 & 0 & 0 & 0 & 0 & 0 & \varepsilon_u & 0 & 0 & 0 & 0 \\ 0 & 0 & 0 & 0 & 0 & 0 & 0 & 0 & 0 & 0 & 0 & 0 & \varepsilon_v & 0 & 0 & 0 \\ 0 & 0 & 0 & 0 & 0 & 0 & 0 & 0 & 0 & 0 & 0 & 0 & 0 & \varepsilon_v & 0 & 0 \\ 0 & 0 & 0 & 0 & 0 & 0 & 0 & 0 & 0 & 0 & 0 & 0 & 0 & 0 & \varepsilon_u & 0 \\ 0 & 0 & 0 & 0 & 0 & 0 & 0 & 0 & 0 & 0 & 0 & 0 & 0 & 0 & 0 & \varepsilon_u \end{bmatrix}.$$

APPENDIX C: NOTATION

A, E, ρ, L	cross-sectional area, Young's modulus, density and length of the shaft
i	$=\sqrt{-1}$
e	$=2{\cdot}71828$
I^d, Δ^d, J^d	average, deviatoric and polar disk moment of inertia
I^d_μ, I^d_v	second moment of inertia about the principal axes μ and v of the disk
K, C	stiffness and damping coefficients of bearing
k, ζ	non-dimensional K, C
m^d	mass of disk
$[M(Z)]$	matrix of shaft shape function
$\mathscr{M}, \mathscr{N}$	bending moments in the rotating frame
M, N	non-dimensional $\mathscr{M}, \mathscr{N}$

$\mathscr{P}', \mathscr{Q}'$	shear forces in the fixed frame
$\mathscr{P}, \mathscr{Q}$	shear forces in the rotating frame
P, Q	non-dimensional $\mathscr{P}, \mathscr{Q}$
$\{r\}, \{R\}$	non-dimensional displacement vector and amplitude function related to (UVW)
$\{\mathbf{S}\}$	state vector
$[\mathbf{T}]$	transfer matrix
U, V	lateral deflections in the rotating frame
u, v	non-dimensional U, V
(UVW)	the rotating frame or principal axes of shaft
$\{W\}$	column vector of constant coefficients
w	real constant coefficients
(XYZ)	the fixed frame of reference
X, Y	lateral deflections in the fixed frame
Z, t	position and time co-ordinates
α, β	deflected angle components in the rotating frame (UVW)
Ψ, Δ	average and deviatoric moment of area of shaft
Ψ_u, Ψ_v	second moment of area about the principal axes U and V of shaft
ε	$\Delta/\Psi = (\Psi_u - \Psi_v)/(\Psi_u + \Psi_v)$
ε_v	$= \Psi_v/\Psi$
ε_u	$= \Psi_u/\Psi$
σ	eigenvalue of shape function of shaft
Ω	rotating speed
Ω_0	fundamental speed
τ	$= \Omega_0 t$, non-dimensional time
γ	$= \Omega/\Omega_0$, non-dimensional rotating speed
ω	non-dimensional whirl frequency
(μv)	principal axes of a non-axisymmetrical disk
$\{\mathfrak{R}_0\}, \{\mathfrak{R}_n\}$	vectors of shape functions with derivatives

Superscripts

T	transpose of a vector or a matrix
s, d, b, o	shaft, disk, bearing, overall system

Subscripts

c, s	cosine or sine term
R, L	the right and left side of a whole rotor
r, l	the right and left side of a component of a rotor
n	the number of the harmonic order